Structure and Bonding of d^8 Allyl Complexes $M(\eta^3\text{-allyl})L_3$ (M = Co, Rh, Ir; L = Phosphine or Carbonyl)

Alireza Ariafard and Zhenyang Lin*

Department of Chemistry and Open Laboratory of Chirotechnology of the Institute of Molecular Technology for Drug Discovery and Synthesis, The Hong Kong University of Science and Technology, Clear Water Bay, Kowloon, Hong Kong

Received April 6, 2005

Density functional theory calculations were used to study structure and bonding of d^8 five-coordinate allyl complexes $M(\eta^3\text{-allyl})L_3$ (M = Co, Rh, Ir; L = phosphine or carbonyl). In these pseudo-square-pyramidal d^8 complexes, we found that only the exo structures correspond to energy minima on the potential energy surface. The exo structures are able to maximize the metal(d)-to-allyl(π^*) back-bonding interaction. The calculations predicted that the endo structures for the Ir and Co complexes are transition states for interconversion of two different exo structures. Complexes such as $Ir(\eta^3\text{-allyl})(PMe_3)_3$ having only phosphines as the ancillary ligands possess the strongest metal−allyl bonding interaction, while complexes such as $Co(\eta^3\text{-allyl})(CO)_3$ having only carbonyls have the weakest interactions. We also studied the $\eta^3 \rightarrow \eta^3 \rightarrow \eta^3$ and $\eta^3 \rightarrow \eta^1 \rightarrow \eta^3$ rearrangements of the allyl ligand and found that both the rearrangement mechanisms are energetically feasible for the d^8 complexes studied in this paper.

Introduction

During the past three decades, η^3-allyl metal complexes have attracted considerable interest both experimentally[1] and theoretically.[2] It is well known that a given η^3-allyl complex can adopt endo and exo isomers depending on the orientation of the substituent on the central carbon of the η^3-allyl moiety with respect to a defined unique ligand in the metal fragment. In the endo isomer, the substituent points away from the unique ligand; in the exo isomer, the substituent points toward from the unique ligand. Extensive studies showed that for many complexes both endo and exo isomers can be simultaneously present in solution although one isomer can be relatively more stable than the other. For instance, for the d^6 complexes $Ru(\eta^3\text{-allyl})X(CO)L_2$ [3] and the d^4 complexes $CpRuX_2(\eta^3\text{-allyl})$[4] (Scheme 1), where L and X are phosphines and halides, respectively, endo isomers were found to be more stable than their exo isomers and NMR studies indicate that both the exo and endo isomers are observable in solution. In the d^6 complexes, X is considered as the unique ligand for the definition of the endo and exo isomers. In the d^4 complexes, Cp is considered as the unique ligand. Interestingly, for the d^8 five-coordinate complexes $M(\eta^3\text{-allyl})L_3$ (Scheme 1) (M = Co, Rh, Ir; L = phosphine or carbonyl),[5−8] which adopt square pyramidal structures (SQP) if η^3-allyl is considered as a pseudo-bidentate ligand, exo isomers are the only conformers that exist in solution. Here, we use the empty coordination site as the reference in defining the endo and exo isomers. Using an empty coordination site as the reference is for the purpose of correlating the exo structures of the d^6 and d^8 complexes (see Scheme 1).

* To whom correspondence should be addressed. E-mail: chzlin@ust.hk.

(1) See for example: (a) Kondo, H.; Yamaguchi, Y.; Nagashima, H. *Chem. Commun*. **2000**, 1075. (b) Liu, G.; Beetstra, D. J.; Meetsma, A.; Hessen, B. *Organometallics* **2004**, *23*, 3914. (c) Borgmann, C.; Limberg, C.; Kaifer, E.; Pritzkow, H.; Zsolnai, L. *J. Organomet. Chem.* **1999**, *580*, 214. (d) Matsushima, Y.; Onitsuka, K.; Takahashi, S. *Organometallics* **2004**, *23*, 3763. (e) Yih, K. H.; Lee, G. H.; Huang, S. L.; Wang, Y. *Organometallics* **2002**, *21*, 5767. (f) Wakefield, J. B.; Stryker, J. *Organometallics* **1990**, *9*, 2428. (g) van Staveren, D. R.; Weyhermüller, T.; Metzler-Nolte, N. *Organometallics* **2000**, *19*, 3730. (h) Faller, J. W.; Chen, C.-C.; Mattina, M. J.; Jakubowski, A. *J. Organomet. Chem.* **1973**, *52*, 361. (i) Cosford, D. P. N.; Liebeskind, L. S. *Organometallics* **1994**, *13*, 1498. (j) Ascenso, J. R.; Dias, R. A.; Fernandes, J. A.; Martins A. M.; Rodrigues S. S. *Inorg. Chim. Acta* **2003**, *356*, 279. (k) Albers, M. O.; Liles, D. C.; Robinson, D. J.; Shaver, A.; Singleton, E. *Organometallics* **1987**, *6*, 2347. (l) McGhee, W. D.; Bergman, R. C. *J. Am. Chem. Soc.* **1988**, *110*, 4246. (m) Gibson, D. H.; Hsu, W.-L.; Steinmetz, A. L.; Johnson, B. V. *J. Organomet. Chem.* **1981**, *208*, 89.

(2) (a) Cedeño, L. D.; Weitz, E. *Organometallics* **2003**, *22*, 2652. (b) Swang, O.; Blom, R. *J. Organomet. Chem.* **1998**, *561*, 29. (c) Tobisch, S.; Taube, R. *Organometallics* **1999**, *18*, 3045. (d) Suzuki, T.; Okada, G.; Hioki, Y.; Fujimoto, H. *Organometallics* **2003**, *22*, 3649. (e) Clot, E.; Eisenstein, O.; Weng, T. S.; Penner-Hahn, J.; Caulton, K. G. *J. Am. Chem. Soc.* **2004**, *126*, 9079. (f) Solin, N.; Szabó, I. *Organometallics* **2001**, *20*, 5464. (g) Schilling, B. E. R.; Hoffmann, R.; Faller, J. W. *J. Am. Chem. Soc.* **1979**, *101*, 592. (h) Webster, C. E.; Hall, M. B. *Organometallics* **2001**, *20*, 5606. (i) Curtis, M. D.; Eisenstein, O. *Organometallics* **1984**, *3*, 887. (j) Carfagna, C.; Galarini, R.; Linn, K.; López, J. A.; Mealli, C.; Musco, A. *Organometallics* **1993**, *12*, 3019.

(3) (a) Xue, P.; Bi, S.; Sung, H. H. Y.; Williams, I. D.; Lin, Z.; Jia, G. *Organometallics* **2004**, *23*, 4735. (b) Sasabe, H.; Nakanishi, S.; Takata, T. *Inorg. Chem. Commun*. **2002**, *5*, 177. (c) Hiraki, K.; Matsunaga, T.; Kawano, H. *Organometallics* **1994**, *13*, 1878. (d) Hill, A. F.; Ho, C. T.; Wilton-Ely, D. E. T. *Chem. Commun*. **1997**, 2207. (e) Hiraki, K.; Ochi, N.; Sasada, Y.; Hayashida, H.; Fuchita, Y.; Yamanaka, S. *J. Chem. Soc., Dalton Trans*. **1985**, 873. (f) Barnard, C. F. J.; Daniels, B. J. A.; Holland, P. R.; Mawby, R. J. *J. Chem. Soc., Dalton Trans*. **1980**, 2418. (g) Cadierno, V.; Crochet, P.; Diez, J.; Garcia-Garrido, S. E.; Gimeno, J. *Organometallics* **2003**, *22*, 5226.

(4) (a) Albers, M. O.; Liles, D. C.; Robinson, D. J.; Shaver, A.; Singleton, E. *Organometallics* **1987**, *6*, 2347. (b) Hubbard, J. L.; Zoch, C. R. *J. Organomet. Chem.* **1995**, *487*, 65. (c) Itoh, K.; Fukahori, T. *J. Organomet. Chem.* **1988**, *349*, 227. (d) Nagashima, H.; Mukai, K.; Shiota, Y.; Yamaguchi, K.; Ara, K. I.; Fukahori, T.; Suzuki, H.; Akita, M.; Moro-oka, Y.; Itoh, K. *Organometallics* **1990**, *9*, 799. (e) Gemel, C.; Mereiter, K.; Schmid, R.; Kirchner, K. *Organometallics* **1996**, *15*, 532.

10.1021/om050257b CCC: $30.25
Publication on Web 06/16/2005

Scheme 1

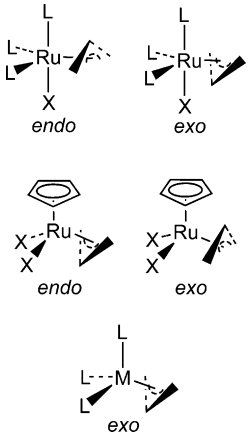

The different isomerism behaviors can be easily deduced by comparing the ^{31}P NMR spectra at low temperature of the d^8 complex Ir(η^3-$CH_2CHCHC_6H_4Me$-*p*)$CO(PPh_3)_2$[6d] and the d^6 complex Ru(η^3-CH_2CHCMe_2)Cl(CO)$(PPh_3)_2$.[3a] The ^{31}P NMR spectrum of the former exhibits two sharp doublets at 207 K, while the spectrum of the latter possesses four peaks at 242 K. Continuing our interest in η^3-allyl complexes,[3a,9] in this article we present our structure and bonding studies on the d^8 five-coordinate complexes M(η^3-allyl)L_3 (**3**) (M = Co, Rh, Ir; L = phosphine *or* carbonyl). We will answer the question why endo isomers are not stable in these d^8 M(η^3-allyl)-L_3 complexes with the aid of density functional theory calculations. In addition, the η^3-allyl rearrangement processes, which are important in understanding the fluxionality behavior in this class of complexes, will also be investigated.

Computational Details

Gaussian 03[10] was used to fully optimize all structures at the B3LYP level of theory,[11] and then frequencies were analytically computed at the same level to confirm whether the structures are minima or transition states, as appropriate. The effective core potentials of Hay and Wadt with double-ζ valance basis sets (LanL2DZ)[12] were chosen to describe Co, Rh, and Ir. The 6-31G basis set was used for the C, H, and O atoms. Polarization functions were also added for C ($\zeta_d = 0.6$), O ($\zeta_d = 1.154$), P ($\zeta_d = 0.340$), Co ($\zeta_f = 2.780$), Rh ($\zeta_f = 1.350$), and Ir ($\zeta_f = 0.938$).[13,14] Calculations of intrinsic reaction coordinates (IRC)[15] were also performed on transition states to confirm that such structures are indeed connecting two minima. Molecular orbitals obtained from the B3LYP calculations were plotted using the Molden 3.7 program written by Schaftenaar.[16]

Results and Discussion

As mentioned in the Introduction, the most important aim of this work is to investigate why exo isomers of the d^8 complexes M(η^3-allyl)L_3 are the only conformers that were observed experimentally. To understand this unique feature and the bonding in this class of complexes, calculations were carried out on the model complexes Ir(η^3-allyl)$(PMe_3)_3$ (**1**), Ir(η^3-allyl)$(CO)_3$ (**2**), Rh(η^3-allyl)$(CO)_3$ (**3**) Co(η^3-allyl)$(CO)_3$ (**4**), Ir(η^3-allyl)-$(CO)(PMe_3)_2$ (**5**), Rh(η^3-allyl)$(CO)(PMe_3)_2$ (**6**), Ir(η^3-allyl)-$(CO)_2(PMe_3)$ (**7**), and Co(η^3-allyl)$(CO)_2(PMe_3)$ (**8**). Figures 1 and 2 show the optimized geometries for complexes **1**−**8**.

The results of the calculations indicate that, regardless what the ancillary ligands L and the metal centers are, for all the model complexes, the exo structures correspond to energy minima on the potential energy surface (PES). The endo structures, which will be discussed later, are not local minima on the PES and the majority of them are transition states for interconversion of two different exo structures having different apical ligands.

Structures of M(η^3-allyl)L_3 (M = Ir, Rh, Co; L = PMe_3 or CO). Let us start our discussion with the allyl complexes having phosphines, Ir(η^3-allyl)$(PMe_3)_3$ (**1**), or carbonyls, M(η^3-allyl)$(CO)_3$ (M = Ir (**2**), Rh (**3**), Co (**4**)), as the ancillary ligands (Figure 1). Figure 1 shows all the calculated structures. Consistent with the general observation, the η^3-ally ligands in the calculated struc-

(5) (a) Thompson, M. R.; Day, V. W.; David Tau, K.; Muetterties, E. L. *Inorg. Chem.* **1981**, *20*, 1237. (b) Bleeke, J. R.; Peng, W. J. *Organometallics* **1984**, *3*, 1422. (c) Merola, J. S.; Kacmarcik, R. T.; Van Engen, D. *J. Am. Chem. Soc.* **1986**, *108*, 329. (d) Bleeke, J. R.; Peng W. J. *Organometallics* **1986**, *5*, 635. (e) Bleeke, J. R.; Donnay, E.; Rath, N. P. *Organometallics* **2002**, *21*, 4099. (f) Bleeke, J. R.; Luaders, S. T.; Robinson, K. D. *Organometallics* **1994**, *13*, 1592. (g) Bleeke, J. R.; Haile, T.; New, P. R.; Chiang, M. Y. *Organometallics* **1993**, *12*, 517. (h) Klein, H.-F.; Auer, E.; Jung, T.; Roehr, C. *Organometallics* **1995**, *14*, 2725.

(6) (a) Manger, M.; Wolf, J.; Teichert, M.; Stalke, D.; Werner, H. *Organometallics* **1998**, *17*, 3210. (b) Choi, J.-C.; Osakada, K.; Yamamoto, T. *Organometallics* **1998**, *17*, 3044. (c) Bleeke, J. R.; Boorsma, D.; Chiang, M. Y.; Clayton, T. W.; Haile, T., Jr.; Beatty, A. M.; Xie, Y. F. *Organometallics* **1991**, *10*, 2391. (d) Osakada, K.; Kimura, M.; Choi, J.-C. *J. Organomet. Chem.* **2000**, *602*, 144. (e) Osakada, K.; Choi, J.-C.; Koizumi, T.; Yamaguchi, I.; Yamamoto, T. *Organometallics* **1995**, *14*, 4962.

(7) (a) Rinze, P. V.; Muller, U. *Chem. Ber.* **1979**, *112*, 1973. (b) Cann, K.; Riley, P. E.; Davis, R. E.; Pettit, R. Inorg. Chem. **1978**, *17*, 1421. (c) Lee, G.-H.; Peng, S.-M.; Liao, M.-Y.; Liu, R.-S. *J. Organomet. Chem.* **1986**, *312*, 113. (d) Stokes, H. L.; Smalley, T. L.; Hunter, M.; Welker, M. E.; Rheingold, A. L. *Inorg. Chim. Acta* **1994**, *220*, 305. (e) Loubser, C.; Roos, H. M.; Lotz, S. *J. Organomet. Chem.* **1991**, *402*, 393.

(8) (a) Lentz, D.; Willemse, S. *Angew. Chem., Int. Ed.* **2001**, *40*, 2087. (b) Hitchcock, P. B.; Mason, R. *Chem. Commun.* **1966**, 503. (c) Beers, O. C. P.; Elsevier, C. J.; Ernsting, J. M.; De Ridder, D. J. A.; Stam, C. H. *Organometallics* **1992**, *11*, 3886. (d) Sovago, J.; Newton, M. G.; Mushina, E. A.; Ungvary, F. *J. Am. Chem. Soc.* **1996**, *118*, 9589.

(9) (a) Bi, S.; Ariafard, A.; Jia, G.; Lin, Z. *Organometallics* **2005**, *24*, 680. (b) Ariafard, A.; Bi, S.; Lin, Z. *Organometallics* **2005**, *24*, 2241.

(10) Frisch, M. J.; Trucks, G. W.; Schlegel, H. B.; Scuseria, G. E.; Robb, M. A.; Cheeseman, J. R.; Montgomery, J. A.; Vreven, T., Jr.; Kudin, K. N.; Burant, J. C.; Millam, J. M.; Iyengar, S. S.; Tomasi, J.; Barone, V.; Mennucci, B.; Cossi, M.; Scalmani, G.; Rega, N.; Petersson, G. A.; Nakatsuji, H.; Hada, M.; Ehara, M.; Toyota, K.; Fukuda, R.; Hasegawa, J.; Ishida, M.; Nakajima, T.; Honda, Y.; Kitao, O.; Nakai, H.; Klene, M.; Li, X.; Knox, J. E.; Hratchian, H. P.; Cross, J. B.; Adamo, C.; Jaramillo, J.; Gomperts, R.; Stratmann, R. E.; Yazyev, O.; Austin, A. J.; Cammi, R.; Pomelli, C.; Ochterski, J. W.; Ayala, P. Y.; Morokuma, K.; Voth, G. A.; Salvador, P.; Dannenberg, J. J.; Zakrzewski, V. G.; Dapprich, S.; Daniels, A. D.; Strain, M. C.; Farkas, O.; Malick, D. K.; Rabuck, A. D.; Raghavachari, K.; Foresman, J. B.; Ortiz, J. V.; Cui, Q.; Baboul, A. G.; Clifford, S.; Cioslowski, J.; Stefanov, B. B.; Liu, G.; Liashenko, A.; Piskorz, P.; Komaromi, I.; Martin, R. L.; Fox, D. J.; Keith, T.; Al-Laham, M. A.; Peng, C. Y.; Nanayakkara, A.; Challacombe, M.; Gill, P. M. W.; Johnson, B.; Chen, W.; Wong, M. W.; Gonzalez, C.; Pople, J. A. *Gaussian 03*, revision B05; Gaussian, Inc.: Pittsburgh, PA, 2003.

(11) (a) Becke, A. D. *J. Chem. Phys.* **1993**, *98*, 5648. (b) Miehlich, B.; Savin, A.; Stoll, H.; Preuss, H. *Chem. Phys. Lett.* **1989**, *157*, 200. (c) Lee, C.; Yang, W.; Parr, G. *Phys. Rev.* **1988**, *B37*, 785.

(12) (a) Hay, P. J.; Wadt W. R. *J. Chem. Phys.* **1985**, *82*, 270. (b) Wadt, W. R.; Hay, P. J. *J. Chem. Phys.* **1985**, *82*, 284. (c) Hay, P. J.; Wadt, W. R. *J. Chem. Phys.* **1985**, *82*, 299.

(13) Huzinaga, S. *Gaussian Basis Sets for Molecular Calculations*; Elsevier Science Pub. Co.: Amsterdam, 1984.

(14) Ehlers, A. W.; Bohme, M.; Dapprich, S.; Gobbi, A.; Hollwarth, A.; Jonas, V.; Kohler, K. F.; Stegmann, R.; Veldkamp, A.; Frenking, G. *Chem. Phys. Lett.* **1993**, *208*, 111.

(15) (a) Fukui, K. *J. Phys. Chem.* **1970**, *74*, 4161. (b) Fukui, K. *Acc. Chem. Res.* **1981**, *14*, 363.

(16) Schaftenaar, G. *Molden* v3.7; CAOS/CAMM Center Nijmegen: Toernooiveld, Nijmegen, Netherlands, 2001.

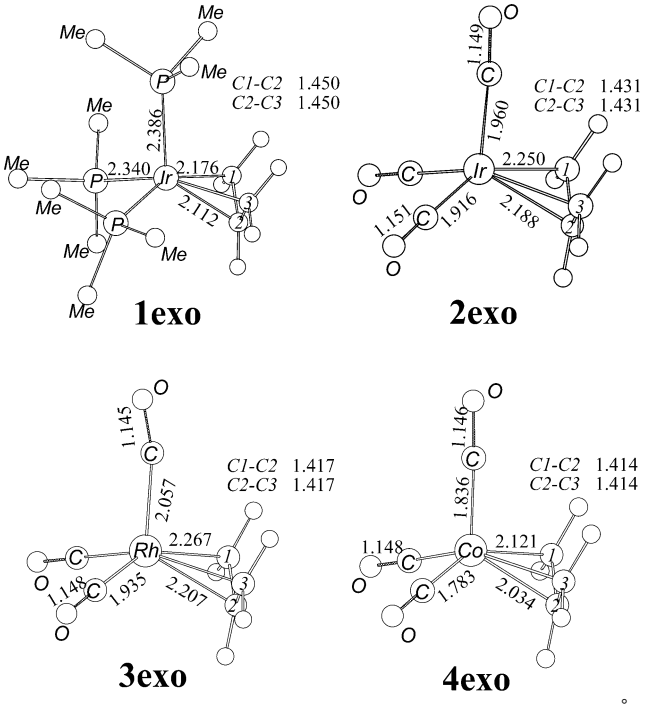

Figure 1. Selected calculated structural parameters (Å) for Ir(η^3-allyl)(PMe_3)$_3$ (**1**), Ir(η^3-allyl)(CO)$_3$ (**2**), Rh(η^3-allyl)-(CO)$_3$ (**3**), and Co(η^3-allyl)(CO)$_3$ (**4**).

tures are all in the exo arrangement. From Figure 1, we can see that the apical M−L distances of all the complexes are longer than the basal M−L distances. The same trend was found experimentally for Ir(η^3-CH_2-CHCHCHO)(PMe_2Ph)$_3$ (2.316(2) vs 2.263(3) Å av),[5g] Ir-(η^3-CH_2CHCHCH=NCMe$_3$)(PMe_3)$_3$ (2.289(2) vs 2.251(3) Å av),[5f] and {Co[η^3-CH_2C(CH_2)CH_2](CO)$_3$}$_2$ (1.815(2) vs 1.769(2) Å av).[7b] In contrast, many 16-electron complexes adopting square pyramidal structures have shorter apical M−L bonds as compared with their basal M−L bonds. For instance, the 16-electron boryl complex RhCl-(PPh_3)$_2$(Bcat)$_2$ adopting a SQP structure has the apical Rh−B bond shorter than the basal Rh−B bond.[17,18]

Calculations on M(η^3-allyl)(CO)(PMe_3)$_2$ (M = Ir (**5**), Rh (**6**)) and M(η^3-allyl)(CO)$_2$(PMe_3) (M = Ir (**7**), Co (**8**)) were also carried out to show how the relative arrangement of the ancillary ligands affects the stability of the structures. The optimized structures, which are all in the exo form, of these complexes are depicted in Figure 2. In agreement with experimental findings, the most favored coordination site of the carbonyl ligand in **5** or **6** is the basal position; that is, **5exo1** or **6exo1** is the most stable structure. **5exo2** and **6exo2**, each having a carbonyl ligand occupying the apical position, are ca. 4.0 kcal/mol less stable than **5exo1** and **6exo1**, respectively. For **7**, similar to the site preference found in **5** and **6**, the carbonyl ligands also prefer to occupy the basal sites. In contrast, in the most stable structure of **8**, one of the carbonyl ligands prefers the apical position, although the energy difference between **8exo1** and **8exo2** is quite small (0.3 kcal/mol). The site preference predicted for the most stable structure of **8** is in agreement with the experimental finding that Co(η^3-

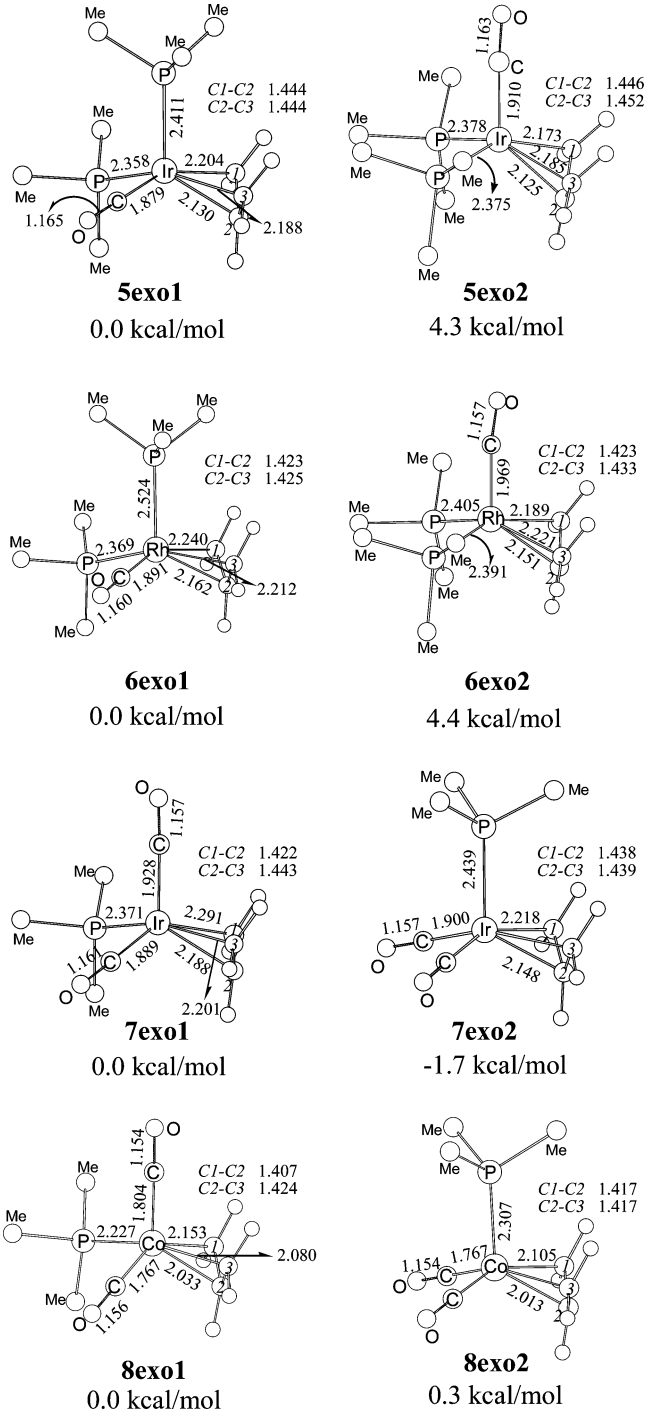

Figure 2. Selected calculated structural parameters (Å) for Ir(η^3-allyl)(CO)(PMe_3)$_2$ (**5**), Rh(η^3-allyl)(CO)(PMe_3)$_2$ (**6**), Ir(η^3-allyl)(CO)$_2$$PMe_3$ (**7**), and Co(η^3-allyl)(CO)$_2$$PMe_3$ (**8**).

allyl)(CO)$_2$(PPh_3)[7a] adopts the **8exo1** structure. In all these complexes, similar to what has been seen for **1exo**−**4exo**, for a given complex, the apical M−L distance is longer than the basal M−L distance. The trend is observed in M(η^3-CH_2CHCH-*p*-C_6H_4Me)(CO)-(PPh_3)$_2$ (M = Ir and Rh)[6b,d] and Co(η^3-allyl)(CO)$_2$-(PPh_3).[7a] The experimental values are Ir−P(apical) = 2.365(5) Å, Ir−P(basal) = 2.299(4) Å, Rh−P(apical) = 2.443(2) Å, and Rh−P(basal) = 2.318(2) Å for M(η^3-CH_2-CHCH-*p*-C_6H_4Me)(CO)(PPh_3)$_2$ (M = Ir and Rh) and Co−CO(apical) = 1.780(5) Å and Co−CO(basal) = 1.758(3) Å for Co(η^3-allyl)(CO)$_2$(PPh_3).

(17) Lam, K. C.; Lam, W. H.; Lin Z.; Marder, T. B.; Norman, N. C. *Inorg. Chem*. **2004**, *43*, 2541.
(18) Baker, R. T.; Calabrese, J. C.; Westcott, S. A.; Neguyen, P.; Marder, T. B. *J. Am. Chem. Soc.* **1993**, *115*, 4367.

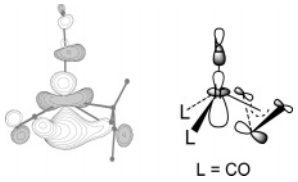

Figure 3. Spatial plot of the highest occupied molecular orbital of Ir(η^3-allyl)(CO)$_3$ (**2**).

Bonding Model. To understand the reason all the complexes studied here adopt exo structures, it is necessary to consider their electronic structures. The complexes studied here are all 18-electron complexes. As mentioned in the Introduction, these complexes can be described as having square pyramidal structures. For an 18-electron square pyramidal ML_5 complex, there are four frontier molecular orbitals available for the eight metal d electrons. These four orbitals are commonly known as "t_{2g}" set orbitals and an s−p−d hybridized a_1 orbital.[19] The a_1 orbital has the maximum amplitude in the direction opposite the M−L(apical) bond and is slightly antibonding with the apical ligand. Because of its antibonding character and hybridization with the high lying s and p orbitals, the a_1 orbital is always found as the HOMO. Compared to the "t_{2g}" set orbitals, the a_1 orbital lies relatively high in energy. Therefore, the optimal arrangement of the allyl ligand is the one in which the a_1 orbital can be effectively stabilized. Figure 3 shows the spatial plot of the a_1 orbital for Ir(η^3-allyl)(CO)$_3$ (**2**) which defines the HOMO in these d^8 complexes. From the HOMO shown in Figure 3, we can see that the π^* orbital of the allyl ligand is used to stabilize the a_1 orbital through a metal(d)-to-allyl(π^*) back-bonding interaction. It is now clear that an endo arrangement of the allyl ligand will turn off the back-bonding interaction and becomes less preferred. Figure 3 also shows the M−L(apical) antibonding character in the a_1 orbital as discussed above. The antibonding character in the a_1 orbital (HOMO) also explains why the apical bond is always weaker than the basal bonds.

It should be pointed out here that in the literature the bonding for Co(η^3-allyl)(CO)$_3$ was well discussed on the basis of a structure having the π-allyl ligand at the top of a C_{3v}-Co(CO)$_3$ fragment.[20,21] The bonding analysis was also able to explain the preferred exo conformation as pointed out above. Examining the structures of many d^8 M(η^3-allyl)L$_3$ complexes, we feel that these allyl complexes are best described as having SQP structures because an allyl ligand is normally considered to occupy two ligand sites. An SQP description can adequately distinguish the apical and basal M−L bonds, which were particularly emphasized in the preceding section.

Ligand Site Preference. In view of the structures calculated for complexes **5** and **6** (Figure 2), we can come to a conclusion that the carbonyl ligand in each of the two complexes prefers to occupy one of the basal positions. This is understandable because it can help stabilize the a_1 orbital through back-bonding interaction (Figure 3). For complexes **7** and **8**, each having two carbonyl ligands, interesting results were obtained. For **7** the two carbonyls prefer being in the basal positions. However, for **8**, the most stable exo structure is the one having only one carbonyl ligand in one of the basal positions. A plausible explanation for the interesting results is given below. Although the carbonyl ligands can help stabilize the a_1 orbital, they also create a situation where they compete against the η^3-allyl ligand for back-bonding. As a result, the competition decreases the stabilizing effect of the carbonyl ligands. For example, in **7**, **7exo2** having two basal carbonyls is more stable than **7exo1** having one basal carbonyl by only 1.7 kcal/mol, smaller than 4.3−4.4 kcal/mol found in **5** and **6**. In **8**, no stabilizing effect can be seen because Co has weaker capability in the back-bonding interactions with π-acid ligands as compared to Ir, evidenced from the calculated CO stretching frequencies (**7exo2**: 2039 and 2087 cm^{-1}; **8exo2**: 2051 and 2089 cm^{-1}).

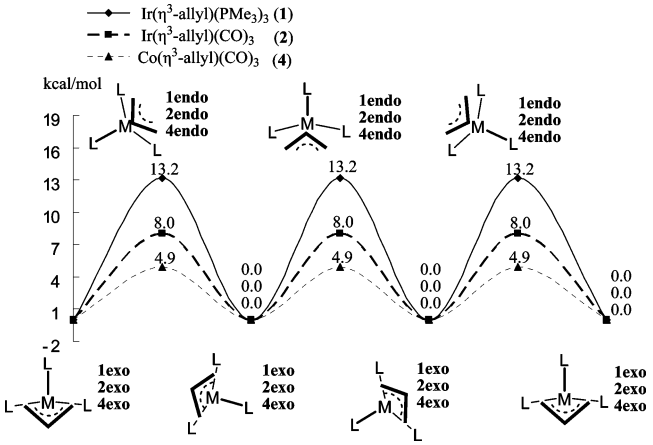

Figure 4. Energy profiles for the rotation of the allyl ligand in complexes **1**, **2**, and **4**.

To illustrate whether steric effects also play a role in the relative stability of the isomers, we also optimized the allyl complexes M(η^3-allyl)(CO)(PH$_3$)$_2$ (M = Ir and Rh) having smaller phosphine ligands. The results indicate that substitution of PH$_3$ for PMe$_3$ does not significantly change the relative stabilities. The exo structures of the Ir(η^3-allyl)(CO)(PH$_3$)$_2$ and Rh(η^3-allyl)(CO)(PH$_3$)$_2$ complexes are 4.0 and 5.1 kcal/mol, respectively, more stable than the corresponding endo structures. The P−Ir−P bond angles of the two different isomers are almost the same, e.g., 104.1° for **5exo1** and 101.2° for **5exo2**. Therefore, the steric effects do not contribute significantly to the relative stability of the exo and endo isomers.

Rotation of the η^3-Allyl Ligand: An $\eta^3 \rightarrow \eta^3 \rightarrow \eta^3$ Pathway. As mentioned above, the calculations indicate that most of the endo structures are transition states on the PES connecting two different exo structures having different apical ligands. Here, it is necessary to see how each endo structure, which is a transition state, connects two different exo isomers. Figures 4 and 5 show the potential energy surfaces connecting the endo and exo structures for some model complexes. From the figures, it is clear that the PES profiles are closely related to the rotation of the η^3-allyl ligand with respect to the metal moiety. The rotation barriers are determined by the energy difference between the relevant exo and endo structures. The results show that the $\eta^3 \rightarrow \eta^3 \rightarrow \eta^3$ rotation barriers are not

(19) Albright, T. A.; Burdett, J. K.; Whangbo, M. H. *Orbital Interactions in Chemistry*; Wiley: New York, 1985.
(20) Albright, T. A.; Hofmann, P.; Hoffmann, R. *J. Am. Chem. Soc.* **1977**, *99*, 7546.
(21) Mingos, D. M. P. In *Comprehensive Organometallic Chemistry*; Pergamon: Oxford, England, 1982; Vol. 3, pp 60−67.

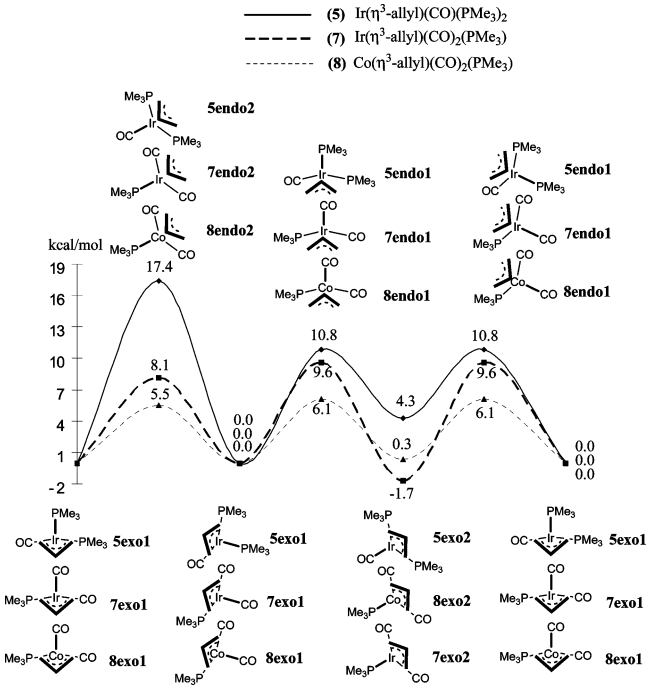

Figure 5. Energy profiles for the rotation of the allyl ligand in complexes **5**, **7**, and **8**.

high for all the complexes studied here, consistent with those predicted in the literature.[20,21]

Figure 4 shows that the rotation barriers calculated for **2** and **4** are lower than those for **1**. The results indicate that complexes having stronger metal−allyl interactions have greater η^3-allyl rotation barriers. The cobalt complex has the smallest rotation barrier because the Co−(η^3-allyl) interaction is expected to be weaker than the Ir−(η^3-allyl) interaction. The weaker Co−(η^3-allyl) interaction can find support from the fact that the cobalt complex has shorter C−C distances in the allyl ligand as compared with the iridium and rhodium complexes. For the two iridium complexes (**1** and **2**), complex **2** has a smaller barrier. Presence of the carbonyl ligand in **2** weakens the Ir−(η^3-allyl) interaction when compared to that in **1**, which does not have a carbonyl ligand competing for the metal(d)-to-ligand-(π^*) back-donation. The structure **1exo** calculated for complex **1** indeed has shorter Ir−C(allyl) bond distances and longer C−C distances in the η^3-allyl ligand than the structure **2exo** calculated for complex **2** (Figure 1), supporting the argument that complex **1** has a stronger Ir−(η^3-allyl) bonding interaction.

Figure 5 shows the calculated rotation barriers for complexes **5**, **7**, and **8**. From Figure 5, it is obvious that, similar to the results reported in Figure 4, the average rotation barrier for each of the three complexes depends on the metal center and the ancillary ligands. Among the three complexes, complex **8** having cobalt as the metal center has the lowest average rotation barrier. **7** having two carbonyl ligands possesses a lower average rotation barrier than **5** having only one carbonyl ligand. Indeed, the greater competition for the metal(d)-to-allyl-(π^*) back-donation between the two carbonyl ligands and the allyl ligand in **7** weakens the metal−allyl bonding interaction and therefore lowers the average barrier. From Figure 5, it is also clear that the endo structures having all the carbonyls in the basal positions, i.e., **5endo1**, **7endo2**, and **8endo2**, are relatively more stable when compared to their other endo isomers. An increase in the number of the strong π-accepting carbonyl ligands in the basal positions seems to stabilize more effectively the a_1 orbital and consequently makes the endo structures relatively more stable.

From Figures 4 and 5, we understand the rotation behavior of the η^3-allyl ligand in complexes **1**, **2**, **4**, **5**, **7**, and **8**. The endo structures for these complexes are the rotation transition states. Interestingly, complexes **3** and **6**, having rhodium as the metal center, behave quite differently. The endo structures of complexes **3** and **6** correspond to neither transition states nor local minima on the PES. For complex **3** or **6**, optimization with an endo structure as the starting geometry always leads to the dissociation of the apical ligand from the metal fragment, no matter what the apical ligand is, CO or PMe_3, giving a square planar $L_2Rh(\eta^3$-allyl) complex and a dissociated ligand. The different behavior of the rhodium complexes is understandable in view of the fact that d^8 square planar rhodium complexes are relatively more prevalent as compared with d^8 square planar iridium complexes and that d^8 square planar cobalt complexes are unknown.

In each of the exo structures of the rhodium complexes, e.g., **3exo**, the apical ligand does not dissociate because the allyl ligand in the exo arrangement is capable of stabilizing the occupied a_1 orbital through the metal(d)-to-allyl(π^*) back-bonding interaction. We calculated the relevant metal−L(apical) bond dissociation energies for M(η^3-allyl)$(CO)_3$ (M = Ir (**2**), Rh (**3**), Co (**4**)). The metal−CO(apical) dissociation energies increase in the order **4** (18.5 kcal/mol) > **2** (12.7 kcal/mol) > **3** (5.4 kcal/mol). This trend supports the fact that the d^8 complexes of Ir and Rh tend to be square planar and that d^8 square planar cobalt complexes do not exist. Since the rhodium complex among the three complexes has the weakest metal−CO(apical) interaction, it is expected that the optimization of its endo structure leads to the dissociation of the apical CO ligand from the metal fragment. Here, we want to emphasize that the trend in the metal−L(apical) bond dissociation energies calculated for **2**−**4** does not have a close correlation with the metal(d)-to-allyl(π^*) back-donation interaction. On the basis of the C−C bond distances in **2**−**4**, we found that Ir−(η^3-allyl) interaction is the strongest among the three complexes, while the metal−η^3-allyl interactions in the cobalt and rhodium complexes (**3** and **4**) are weaker (Figure 1).

$\eta^3 \rightarrow \eta^1 \rightarrow \eta^3$ Rearrangement of the Allyl Ligand. The results above indicated that the rotation barriers of the η^3-allyl ligand with respect to the metal moiety in the model complexes are not high. The NMR studies of Ir(η^3-$CH_2CHCHCH{=}NCMe_3$)$(PMe_3)_3$ established a free energy activation of 11.5 ± 0.4 kcal/mol for the rotation process, which is in good agreement with a barrier of 13.2 kcal/mol calculated for the model complex **1** (Figure 4). Interestingly, the NMR study of Ir(η^3-CH_2-CHCH-*p*-C_6H_4Me)$(CO)(PPh_3)_2$ indicated that instead of $\eta^3 \rightarrow \eta^3 \rightarrow \eta^3$, an $\eta^3 \rightarrow \eta^1 \rightarrow \eta^3$ rearrangement of the allyl ligand is responsible for the observation that the two PPh_3 ligands are equivalent in solution. The experimental result suggests that for Ir(η^3-CH_2CHCH-*p*-

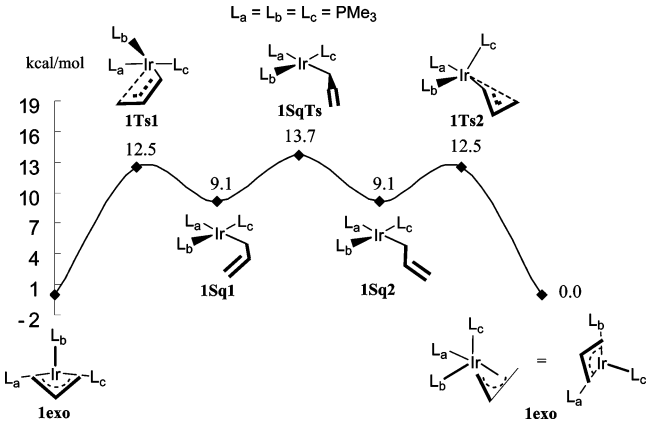

Figure 6. Energy profile for the $\eta^3 \rightarrow \eta^1 \rightarrow \eta^3$ rearrangement of the allyl ligand in complex **1**.

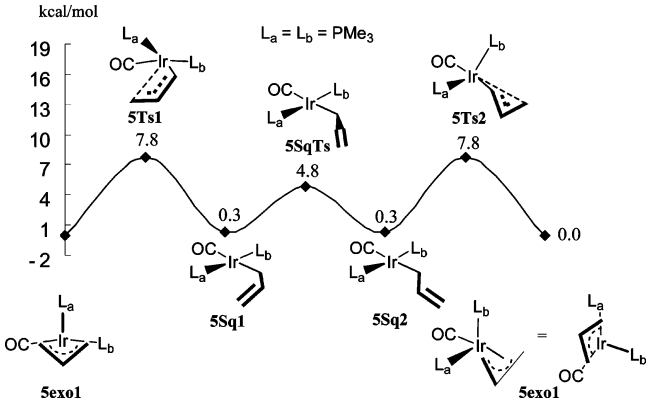

Figure 7. Energy profile for the $\eta^3 \rightarrow \eta^1 \rightarrow \eta^3$ rearrangement of the allyl ligand in complex **5**.

$C_6H_4Me)(CO)(PPh_3)_2$ the $\eta^3 \rightarrow \eta^1 \rightarrow \eta^3$ rearrangement of the allyl ligand should be energetically more favorable than the $\eta^3 \rightarrow \eta^3 \rightarrow \eta^3$ rotation process described in the section above, although the calculations indicate that the $\eta^3 \rightarrow \eta^3 \rightarrow \eta^3$ rotation barrier for Ir(η^3-allyl)(CO)-$(PMe_3)_2$ is not exceedingly high (Figure 5). In this section, we present the results relevant to the $\eta^3 \rightarrow \eta^1 \rightarrow \eta^3$ rearrangement of the allyl ligand for complexes **1** and **5**, the model complexes for Ir(η^3-$CH_2CHCHCH{=}NCMe_3)(PMe_3)_3$ and Ir(η^3-CH_2CHCH-*p*-$C_6H_4Me)(CO)$-$(PPh_3)_2$, respectively.

Figures 6 and 7 show the energy profiles of the $\eta^3 \rightarrow \eta^1 \rightarrow \eta^3$ rearrangement of the allyl ligand for **1** and **5**, respectively. The rearrangement for each complex proceeds through an η^1-allyl intermediate adopting a square planar structure followed by a 180° rotation of the C=C unit within the η^1-allyl ligand and then reformation of the η^3-allyl complex having another phosphine ligand in the apical position. For **1**, the activation barrier of the $\eta^3 \rightarrow \eta^1 \rightarrow \eta^3$ rearrangement (13.7 kcal/mol) (Figure 6) is slightly greater than that for the direct $\eta^3 \rightarrow \eta^3 \rightarrow \eta^3$ rotation (13.2 kcal/mol) (Figure 4). For **5**, the $\eta^3 \rightarrow \eta^1 \rightarrow \eta^3$ rearrangement is however energetically more favorable than the $\eta^3 \rightarrow \eta^3 \rightarrow \eta^3$ rotation [7.8 kcal/mol (Figure 7) vs 17.4 kcal/mol (Figure 5)]. The η^1-allyl intermediate **1Sq1** (or **1Sq2**) is 9.1 kcal/mol higher in energy than the η^3-allyl complex **1exo**. However, **5Sq1** (or **5Sq2**) has stability comparable to **5exo1**. The high stability of **5Sq** relative to **5exo1** explains why the $\eta^3 \rightarrow \eta^1 \rightarrow \eta^3$ rearrangement was observed in Ir(η^3-CH_2-$CHCH$-*p*-$C_6H_4Me)(CO)(PPh_3)_2$. The presence of a carbonyl ligand helps stabilize the square planar intermediate (**5Sq**). The instability of **1Sq** relative to **1exo** makes the barriers high for the $\eta^3 \rightarrow \eta^1 \rightarrow \eta^3$ rearrangement. Therefore, instead of an $\eta^3 \rightarrow \eta^1 \rightarrow \eta^3$ rearrangement, a slightly more favorable $\eta^3 \rightarrow \eta^3 \rightarrow \eta^3$ rotation of the allyl ligand was seen in Ir(η^3-$CH_2CHCHCH{=}NCMe_3)(PMe_3)_3$. The instability of **1Sq** relative to **1exo** can be attributed to the strong metal−η^3-allyl bonding interactions in **1exo**.

Conclusions

Structures and bonding of d^8 five-coordinate η^3-allyl complexes M(η^3-allyl)L_3 (M = Co, Rh, Ir; L = phosphine or carbonyl) have been theoretically investigated. Our studies show that these complexes are structurally better described as square pyramidal when the η^3-allyl ligand is formally considered as a bidentate ligand. We found that the most stable structures are those having the central allylic hydrogen pointing toward the empty coordination site of the square pyramidal geometry, i.e., the exo structures. In a d^8 square pyramidal ML_5 complex, the highest occupied orbital is the a_1 orbital having the maximum amplitude in the empty coordination site. The exo structures gives an optimal metal(d)-to-allyl(π^*) back-bonding interaction that greatly stabilizes the HOMO. In agreement with the experimental findings, for a given complex, the apical M−L distance was found to be longer than the basal ones. The longer apical M−L distance is a result of the HOMO (a_1) having an M−L(apical) antibonding character. Unlike other types of η^3-allyl complexes, the endo structures of the η^3-allyl complexes studied in this article do not correspond to local minima on the PES, again due to the metal−L(apical) slightly antibonding interaction in the HOMO.

For the cobalt and iridium complexes, the endo structures were found to be transition states on the PES connecting two different exo structures having different apical ligands. For the rhodium complexes, an attempt to locate the endo structures resulted in the dissociation of the apical ligand from the metal fragment, giving a square planar structure and the dissociated ligand. The distinct feature of the rhodium complexes is related to the fact that rhodium has the greatest tendency among the triads to form square planar complexes.

In this paper, we have also studied the allyl ligand rearragements. We found that the rotation of the η^3-allyl ligand ($\eta^3 \rightarrow \eta^3 \rightarrow \eta^3$) in these complexes occurs easily, having rotation barriers ranging from 5 to 17 kcal/mol. Because square planar iridium and rhodium complexes are prevalent, the allyl ligand rearrangements in the iridium and rhodium complexes can also proceed easily via an $\eta^3 \rightarrow \eta^1 \rightarrow \eta^3$ mechanism. The barriers are small, ranging from 8 to 14 kcal/mol. These results indicate that both the $\eta^3 \rightarrow \eta^3 \rightarrow \eta^3$ and $\eta^3 \rightarrow \eta^1 \rightarrow \eta^3$ mechanisms are feasible.

Finally we want to point out here that the barriers of the $\eta^3 \rightarrow \eta^1 \rightarrow \eta^3$ allyl ligand rearrangement calculated for the complexes studied in this paper are significantly lower than the $\eta^3 \rightarrow \eta^1 \rightarrow \eta^3$ barriers for Ru(η^3-allyl)-$Cl(CO)(PH_3)_2$ and some other Cp complexes reported earlier.[3a,9] Stable square planar intermediate structures for d^8 Rh and Ir species are responsible for the low $\eta^3 \rightarrow \eta^1 \rightarrow \eta^3$ rearrangement barriers.

Acknowledgment. The authors acknowledge financial support from the Hong Kong Research Grants Council (HKUST 6023/04P and DAG03/04.SC15) and the University Grants Committee of Hong Kong through the Area of Excellence Scheme (Aoe/P-10/01).

Supporting Information Available: Cartesian coordinates for all the calculated structures are available free of charge via the Internet at http://pubs.acs.org.

OM050257B